AP42 Section:	7.1
Related	5
Title:	Emission Measurements on a Floating Roof Pilot Test Tank RJ Laverman, Chicago Bridge & Iron Co. Paper presented at the 44th Refining Midyear Meeting Seesion on API Tanks and Pressure Vessel Technology, May 16, 1979.

Emission Measurements on a Floating Roof Pilot Test Tank

R. J. LAVERMAN, Chicago Bridge & Iron Company,
Plainfield, Illinois

Preprint No. 31-79

A paper presented at the 44th Refining Midyear Meeting
Session on API Tanks & Pressure Vessel Technology
Wednesday, May 16, 1979
San Francisco, California

American Petroleum Institute
2101 L Street, Northwest
Washington, D.C. 20037

CBT-5364

Emission Measurements on a Floating Roof Pilot Test Tank

R. J. LAVERMAN
Chicago Bridge & Iron Company, Plainfield, Illinois

A hydrocarbon evaporation loss measurement program has been performed in a 20 foot diameter pilot floating roof test tank to examine the evaporation loss phenomenon in floating roof tanks. This test tank was a covered floating roof tank through which a controlled flow rate of air was passed. The test tank was calibrated by relating the air flow rate induced pressure variation above the floating roof sealing ring to that which would be expected from an equivalent wind induced pressure variation on a field tank. Direct measurement of the evaporation loss was performed by measuring the total hydrocarbon concentration change in the metered and controlled air flow rate as it passed through the test tank. Parameters thought to affect the evaporation loss rate were systematically varied, and these included: wind speed; product type and vapor pressure; and, seal type and the amount of seal gaps. A proposed vapor pressure function is tested utilizing the evaporation loss data which was measured with variable vapor pressure. The test data is correlated with a proposed evaporation loss equation. The basis for expecting the evaporation losses to scale directly as the diameter of the tank is presented.

so that a controlled quantity of air could be passed between the fixed roof and the floating roof to simulate the affects of wind on an EFRT. In selecting this method, it was realized that it was necessary to establish a relationship between the air flow rate passed through the test tank and the equivalent wind speed over an EFRT.

One of the major advantages in using this method was that one could easily control those variables which were thought to affect the evaporation process, and thus separate the contribution of the different variables. Another advantage was that the emissions would be directly measured with equipment well within the state of the art. Also, the method could be used with a wide range of products, including single component stocks.

2.0 DESCRIPTION OF TEST TANK

The pilot test tank was constructed at CBI's Plainfield, Illinois Research Facility in the spring of 1976. Figure 1 is an overall view, and Figure 2 a simplified schematic of the floating roof pilot test tank. The test tank is 20 ft. in diameter and has a 9 ft. shell height.

The lower 5 ft.-3 in. of the tank shell is provided with a heating/cooling jacket through which a water/ethylene glycol mixture is continuously circulated to control the product at the desired temperature. The portion of the shell extending approximately 1 ft. above this jacketed portion has a separate heating/cooling circulation system, so that the temperature of the shell in this area can be controlled independent of the product temperature to simulate the affect of a heated or cooled rim space shell. The tank shell is externally insulated with a 3 in. thickness of fiberglass blanket, and the tank rests on a 3 in. layer of Foamglas block insulation.

Since it was necessary during the course of the testing program to change the type of floating roof, the fixed roof is provided with a bolting flange so that it can be removed for easy access into the interior of the tank. Personnel access into the test tank is also provided by means of a 30 in. diameter manhole in the fixed roof.

The effect of wind blowing across an EFRT is simulated by means of air which is passed through the space between the floating roof and the fixed roof. The air enters the tank from a blower by means of a 30 in. diameter inlet duct which is connected to an air inlet distribution plenum on one side of the tank. The velocity of the air in the inlet duct is measured with a Flow Technology, Inc., becoming saturated with product vapors in the process. It would then flow vertically upward past the seal, carrying with it product vapors, thus resulting in product emissions.

Marchman measured the pressure coefficient variation over the entire surface of the model floating roof when the roof was at different levels. The pressure coefficient, C_P, is defined as the ratio of the pressure head to the velocity head.

$$C_P \equiv \frac{\left(\frac{P - P_R}{\gamma_A}\right)}{\left(\frac{V^2}{2g}\right)}$$

or

$$C_P = \frac{\left(P - P_R\right)}{\left(\frac{\rho_A V^2}{2g_C}\right)} \qquad (1)$$

Since we are here only interested in the variation of C_P around the floating roof rim, it is useful to look at the variation of the pressure coefficient difference $(C_{PL}-C_P)$, where C_{PL} is the pressure coefficient on the leeward side of the floating roof. Using Equation (1), this difference can be written as:

$$\left(C_{PL} - C_P\right) = \frac{\left(P_L - P\right)}{\left(\frac{\rho_A V^2}{2g_C}\right)} \qquad (2)$$

Thus, for a given wind speed, V, this difference shows essentially how the pressure varies around the floating roof rim relative to the pressure on the leeward side of the floating roof.

Figure 4, which is based on the wind tunnel tests of Marchman, shows how $(C_{PL}-C_P)$ varies around the floating roof rim when the roof is at different levels. Interestingly, the variation with roof level is small, and thus the wind induced emissions would be expected to vary only slightly with roof level. The pressure coefficient difference $(C_{PL}-C_{PW})$ between the leeward and windward side of the floating roof is seen to be approximately 0.93, essentially independent of roof level.

(2). Nonmetallic Vapor-Mounted Primary Seal (CBI Type SR-9 Resilient Foam Fabric Seal) [4,6,7,8]

(3). Nonmetallic Liquid-Mounted Primary Seal (CBI Type SR-5 Liquid Filled Fabric Seal) [14]

A vapor-mounted primary seal is defined as one where there is an annular vapor space of considerable size beneath the seal, and above the liquid surface, which can communicate with any gaps between the tank shell and the seal. The metallic shoe primary seal is not considered to be a vapor-mounted seal since the vapor space between the floating roof rim and the metallic sealing ring is completely enclosed on the top by the continous seal (see Figure 6) and on the bottom by the product. Thus, this vapor space does not communicate directly with any gaps between the tank shell and the metallic sealing ring.

A liquid-mounted primary seal is defined as one where the bottom of the seal contacts and essentially covers the liquid surface between the tank shell and floating roof rim, thus eliminating any large vapor space beneath the seal.

The testing program included tests with and without secondary seals, and included tests where the amount of gaps between the tank shell and both the primary and secondary seal were varied.

One series of tests [10] evaluated the affect of variable continous seal [see Figure 6] tightness. Another series of tests [11] evaluated the affect upon the evaporation rate of simulated rivets in both vertical and girth seam rivet joints.

In addition to varying the types of seals and their conditions, the type of product and its vapor pressure were also varied. The majority of the testing program was performed with a propane/octane mixture, where it was possible to adjust the product vapor pressure by adding propane to this simple mixture. In fact, one series of tests [13] investigated the affect of variable product vapor pressure upon the evaporation rate. Emission tests have been performed with other hydrocarbon mixtures, including gasoline and crude oil [12], and also recently with a single component hydrocarbon, benzene, for the U.S. Environmental Protection Agency (results not yet published).

The affect of the meteorological variables were also investigated. Most of the tests involved varying the simulated wind from approximately 2 to 15 mi/hr since early testing showed that there was a significant affect of the wind upon the evaporation rate. The affect of solar insolation heating of the tank shell in the floating roof rim area was investigated [4, 7], as was also the affect of changing barometric pressure [4]. These later two meteorological variables were observed to have only a minor affect on the evaporation loss for hydrocarbon mixtures, whereas the wind played a major role.

It is interesting to compare the dependency of these two loss equations upon the variables of V, P_v, and D. Each of these variables will now be considered in turn, and where possible, the test data will be utilized to recommend a suitable functional dependency.

5.1 WIND SPEED DEPENDENCY

The wind speed dependency of the emissions may be determined from the slopes of the lines presented in Figures 9 thru 12 for the different seal conditions. The slope, n, or seal wind speed exponent, of each line shown on these figures is presented in Table 2.

Equation (7) was derived for a vapor-mounted primary seal, and predicted a seal wind speed exponent of 2.0. The line on Figure 11 for Tests 13,15,16,20,21,25 and 31, which applies to a vapor-mounted nonmetallic primary seal, has a seal wind speed exponent of 1.2 rather than 2.0, as was predicted in Equation (7). Equation (7) was based on the assumption that the vertical vapor flow past the seal was laminar. A more rigorous derivation [17], based upon measured seal leak tightness test data (which indicated transition rather than laminar flow), yielded an evaporation loss equation similar to Equation (7), but with a seal wind speed exponent of 1.4.

Equation (6) has a wind speed exponent of 0.7, rather than the 2.0 of Equation (7), and thus Equation (6) does not depend as strongly upon wind speed as Equation (7).

The important observation from Figures 9 thru 12, however, is that the slopes of the lines vary considerably with the seal condition, and thus it is not desirable to fix the wind speed exponent at any specific value. Rather, it should be selected for the specific seal condition being considered.

It is interesting to note from Table 2, however, that vapor-mounted seals generally have larger values for the seal wind speed exponent, thus increasing their suseptability to wind driven emissions, which involve flow past the seal and circumferentially around the rim vapor space.

5.2 VAPOR PRESSURE DEPENDENCY

The last term in Equation (6) describes the vapor

The test data is plotted in Figure 14 as emissions versus wind speed. For each vapor pressure, the data was fit with a line, and it was noted that the slopes of all of the lines were essential the same, thus yielding a common wind speed exponent of 1.3.

Utilizing the definition for F, we may write Equation (7) in the following form:

$$L = KM_V DV^2 F \tag{10}$$

As was noted in the Section 5.1, the wind speed exponent varies with the type of seal, and for the seal condition used during the tests shown on Figure 14, a wind speed exponent of 1.3 best fits the test data. Utilizing this wind speed exponent, Equation (10) may be rewritten as follows by dividing both sides by $M_V F$ and converting from L (lbm/yr) to E (lbm/day).

$$\left(\frac{E}{M_V F}\right) = \left(\frac{KD}{365}\right) V^{1.3}$$

$$= SV^{1.3} \tag{11}$$

where S is a constant for all of the tests shown in Figure 14. It was possible to determine S by a least squares fit of the test data, and the resulting value was:

$$S = 0.0734 \ (\pm\ 19.9\ \%\ \text{Standard Deviation}) \tag{12}$$

Figure 15 illustrates how well the correlation of Equation (11) fits the test data with variable vapor pressure.

It is interesting to note that although the vapor function F, defined by Equation (9), was derived specificially for a vapor-mounted primary seal, it correlates the metallic shoe primary seal test data quite well. Thus, it appears to be a good choice for use in a general evaporation loss equation, as will be described in Section 5.4.

5.3 DIAMETER DEPENDENCY

Equation (6) indicates that the evaporation loss depends upon $D^{1.5}$ (for diameters up to 150 ft), whereas Equation (7) indicates that it is directly proportional to D. It is interesting to note that other floating roof tank evaporation loss models [18] have also concluded that the by the API Committee on Evaporation Loss Measurement, Task Group 2517/19 as part of their effort to up-date API Bull. 2517.

5.5 SAMPLE CALCULATIONS

As a example, Equation (13) will be used to estimate the standing-storage evaporation loss for an EFRT 150 ft. in diameter, storing 13 psi RVP gasoline at an average storage temperature of 52°F with different types of sealing systems at wind speeds from 5 to 15 mi/hr.

Assume:

P_V = 6.0 psia
M_V = 56.8 lbm/lbmole
D = 150 ft
V = 5 to 15 mi/hr
K_S = } Values taken from Table 2
n =

Figure 16 shows the estimated evaporation loss, L, versus wind speed, V, for different types of sealing systems.

For comparison, the estimated evaporation loss for a cone roof tank with a 90% efficient vapor recovery system is also shown on Figure 16. This evaporation loss was estimated using API Bull. 2518 [20] for a 150 ft. diameter tank with the same product used above for the conditions of 20F° average daily temperature change, 30 ft. average outage and 8 turnovers per year. The tank roof and shell were assumed to have aluminum color paint in good condition.

Also shown for comparison on Figure 16 is the estimated standing-storage evaporation loss based on API Bull. 2517 for the same conditions as those listed above, where it was further assumed that the tank was aluminum color and of welded construction with a pontoon roof having a single or double tight fitting seal.

Figure 16 demonstrates several trends. It can be seen that evaporation loss estimates based on API Bull. 2517 are considerably larger than those based on the pilot test tank data, thus confirming the need to update this API bulletin. For the three types of primary seals tested, the vapor-mounted nonmetallic primary seal showed the largest evaporation loss. For all three types of primary seals, the use of a rim-mounted secondary seal further significantly

6.0 - CONCLUSIONS

The results of the pilot test tank emission test program lead to conclusions in several areas.

Test Method

- The validity of using the direct emission measurement method in a pilot test tank was demonstrated.
- Using wind induced pressure measurements from both a wind tunnel model and a commercial size EFRT, it was possible to establish a wind speed calibration of the pilot test tank. This calibration related the air flow rate through the pilot test tank to the equivalent wind speed over an EFRT.
- The test method was also evaluated by comparing the directly measured evaporation loss with that simultaneously determined using the indirect product density change method [12].

Test Results

- Evaporation loss estimates based on API Bulletin 2517 are generally considerably larger than those based on the pilot tank tests, thus confirming the need to update the bulletin.
- For the three types of primary seals tested, the evaporation loss from the vapor-mounted nonmetallic primary seal was the highest and also had the highest dependency on wind speed (ie increased faster with increasing wind speed). For nonmetallic seals, the liquid-mounted primary seal performed better than the vapor-mounted primary seal.
- For all three types of primary seals tested, the use of a rim-mounted secondary seal further significantly reduced the evaporation loss on an EFRT. Tests demonstrated that a weather shield was also somewhat effective in reducing the evaporation loss, but not to the extent of a rim-mounted secondary seal.
- The evaporation loss dependency upon the extent of gaps in the primary and/or secondary seal was also evaluated. Of the three types of primary seals tested, gaps were found to most affect the vapor-mounted nonmetallic primary seal, and least affect the metallic shoe primary seal. Supprisingly, however, the evaporation loss was small even with substantial gaps on any primary seal when used with a

REFERENCES

1. U. S. Environmental Protection Agency, "Compliation of Air Pollutant Emission Factors", Supplement No. 7 to AP-42, Section 4.3.2.2, April, 1977.

2. "Evaporation Loss from Floating-Roof Tanks", American Petroleum Institute, Bull. 2517, Feb., 1962.

3. Marchman, J. B. III, "Surface Loading in Open-Top Tanks", Journal of the Structural Division, ASCE Proceedings, Vol. 96, No. ST11, Nov., 1970, pp 2551-2556.

4. Chicago Bridge & Iron Co., "SOHIO/CBI Floating Roof Emission Test Program", Final Report, CBI Research Contract R-0101, Nov. 18, 1976.

5. Chicago Bridge & Iron Co., "Wind Speed Versus Air Flow Rate Calibration of 20 Foot Diameter Floating Roof Test Tank", Final Report, CBI Research Contract R-0177, Oct. 5, 1977.

6. Chicago Bridge & Iron Co., "SOHIO/CBI Floating Roof Emission Test Program", Preliminary Informat-on, CBI Research Contract R-0101, Aug. 27, 1976.

7. Chicago Bridge & Iron Co., "SOHIO/CBI Floating Roof Emission Test Program", Interim Report, CBI Research Contract R-0101, Oct. 7, 1976.

8. Chicago Bridge & Iron Co., "SOHIO/CBI Floating Roof Emission Test Program", Supplemental Report, CBI Research Contract R-0101, Feb. 15, 1977.

9. Chicago Bridge & Iron Co., "Western Oil and Gas Association Metallic Sealing Ring Emission Test Program", Interim Report, CBi Research Contract R-0136, Jan. 19, 1977.

10. Chicago Bridge & Iron Co., "Western Oil and Gas Association Metallic Sealing Ring Emission Test Program", Final Report, CBI Research Contract R-0136, March 25, 1977.

11. Chicago Bridge & Iron Co., "Western Oil and Gas Association Metallic Sealing Ring Emission Test Program", Supplemental Report, CBI Research Contract R-0166, June 30, 1977.

NOMENCLATURE

Symbol	Description	Units
C	Seal leak tightness factor	$\left(\frac{\text{lbmole ft}}{\text{hr lbf}}\right)$
C_P	Pressure coefficient, defined by Eq. (1)	-
D	Tank Diameter	ft
E	Evaporation loss	lbm/day
F	Vapor pressure function, defined by Eq. (9)	-
G	Vapor pressure function, defined by Eq. (8)	-
g	Acceleration due to gravity $(4.17 \times 10^8 \text{ ft/hr}^2)$	ft/hr^2
g_C	Gravitational constant $(4.17 \times 10^8 \text{ lbm sec}^2/\text{lbf ft})$	$\left(\frac{\text{lbm sec}^2}{\text{lbf ft}}\right)$
H	Tank shell height	ft
h	Floating roof level	ft
K	Seal factor, defined by Eq. (A16)	-
K_S	Seal factor for use with Eq. (13), see Table 2	-
L	Evaporation loss	lbm/yr
M	Flow rate vertically between the seal and the tank shell	lbmole/hr
M_V	Molecular weight of the product vapor	lbm/lbmole
n	Seal wind speed exponent, see Table 2	-
P	Pressure	lbf/ft^2
P_V	Product vapor pressure	lbf/in^2
Q	Air flow rate	$\text{sft}^3\text{/min}$
S	Correlation factor in Equation (11)	-
V	Wind speed	ft/hr, or mi/hr

APPENDIX

Derivation Of The Evaporation Loss Equation For A Vapor-Mounted Seal

For the case of vapor-mounted primary seal, it is possible to derive an approximate evaporation loss equation. This derivation is based on the wind induced evaporation loss model described in Section 3.0. The evaporation loss equation derived here can be used to examine how the evaporation loss depends upon the variables of product vapor molecular weight, product vapor pressure, wind speed and tank diameter.

In Section 3.0 it was noted that as the wind flows over an EFRT, a pressure distribution is established above the floating roof rim. As shown in Figure 17, this pressure distribution results in a pressure P_L on the leeward side of the floating roof which is higher than pressure P_W on the windward side of the floating roof. Although the variation of pressure from P_L to P_W above the seal follows the pressure coefficient variation shown in Figures 4 and 5, it will here be assumed for simplicity that the variation is linear, as shown in Figure 17.

The pressure coefficient, C_p, may be defined as follows:

$$C_p \equiv \frac{\left(P - P_R\right)}{\left(\dfrac{\rho_A V^2}{2g_c}\right)} \qquad \text{(A1)}$$

where P_R is the reference air pressure. This equation may be solved for P.

$$P = P_R + C_p\left(\frac{\rho_A V^2}{2g_c}\right) \qquad \text{(A2)}$$

Assuming a linear variation of P from P_L to P_W, we can write:

$$P = P_L - \left(P_L - P_W\right)\left(\frac{\theta}{\pi}\right) \qquad \text{(A3)}$$

where $\left(P_L - P_W\right)$ may be expressed in terms of the pressure coefficient difference $\left(C_{pL} - C_{pW}\right)$ using Equation (A2).

$$M_{AH} = 2\int_{\theta_s}^{\pi} dM_{AH} = C\left(P_L - P_W\right)\left(\frac{D}{2\pi}\right)\left(\pi - \theta_s\right)^2 \qquad \text{(A9)}$$

where the factor 2 is used to account for each side of the floating roof.

Assuming that all the air which enters the rim vapor space becomes saturated with hydrocarbons before it leaves, we may write the following molar rate balance equation for the air entering and leaving the rim vapor space.

$$M_A = y_A\, M_{AH} \qquad \text{(A10)}$$

Subsituting Equations (A8) and (A9) into (A10), we may solve for θ_s.

$$\theta_s = \pi\left(\frac{y_A^{1/2}}{1 + y_A^{1/2}}\right) \qquad \text{(A11)}$$

For an idealized binary mixture of air and hydrocarbon, we may write:

$$y_A = 1 - y_H \qquad \text{(A12)}$$

where the mole faction of hydrocarbon, y_H, may be related to the hydrocarbon vapor pressure, P_V, by the Equation (A13), which is based on Raoult's law.

$$y_H = \left(\frac{P_V}{14.7}\right) \qquad \text{(A13)}$$

From these expressions we see that as P_V approaches 0, θ_s approaches $\pi/2$; and as P_V approaches 14.7, θ_s, approaches 0.

The evaporation loss of hydrocarbons, L (lbm/yr) may be expressed as follows:

$$L = \left(365\ \frac{\text{days}}{\text{yr}}\right)\left(\frac{24\ \text{hr}}{\text{day}}\right) M_V\, y_H\, M_{AH} \qquad \text{(A14)}$$

Substituting Equation (A9) for M_{AH}, we have:

$$L = 8760\, M_V\, y_H\, C\, \left(P_L - P_W\right)\left(\frac{D}{2\pi}\right)\left(\pi - \theta_s\right)^2$$

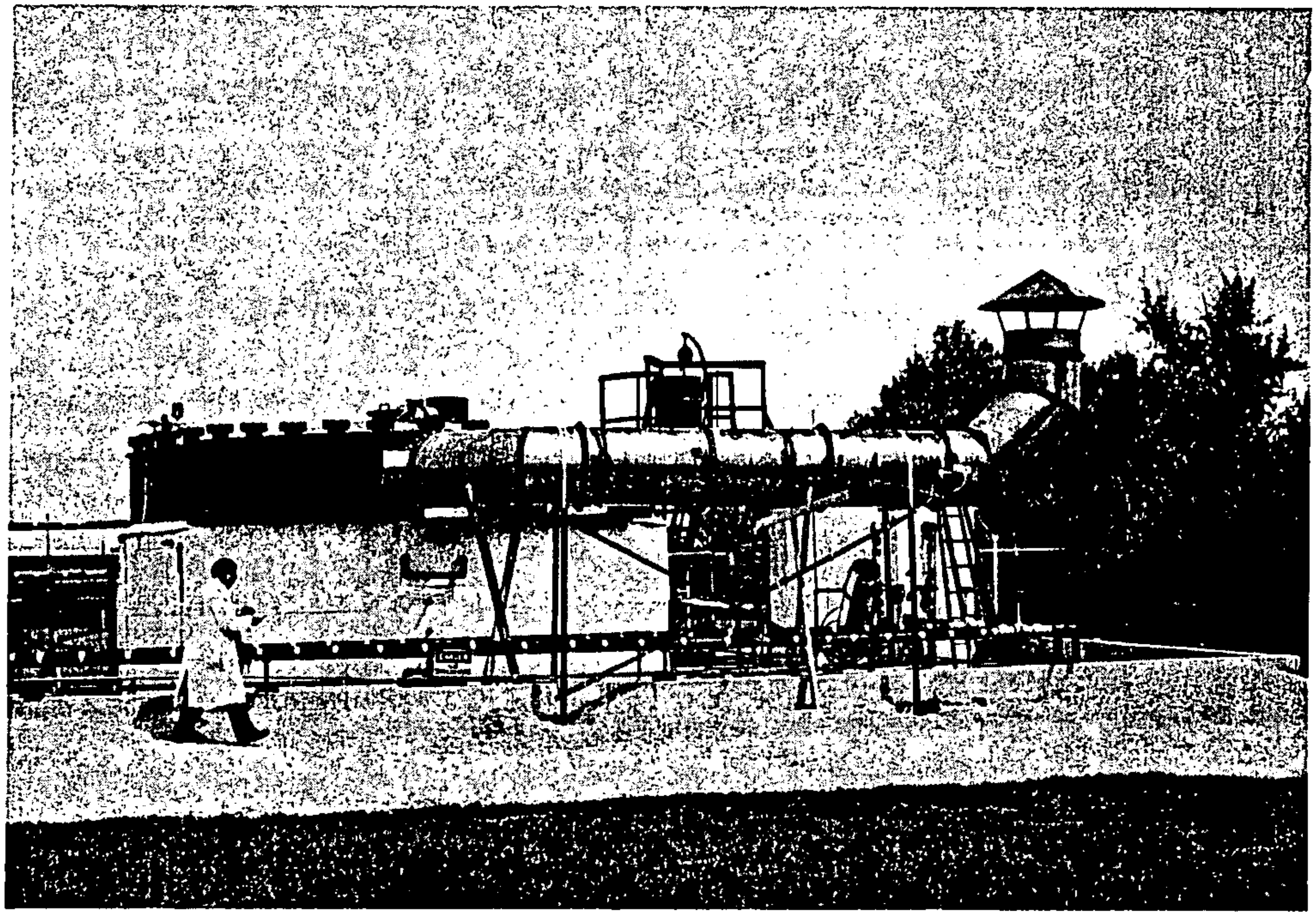

Figure 1 - Floating Roof Pilot Test Tank

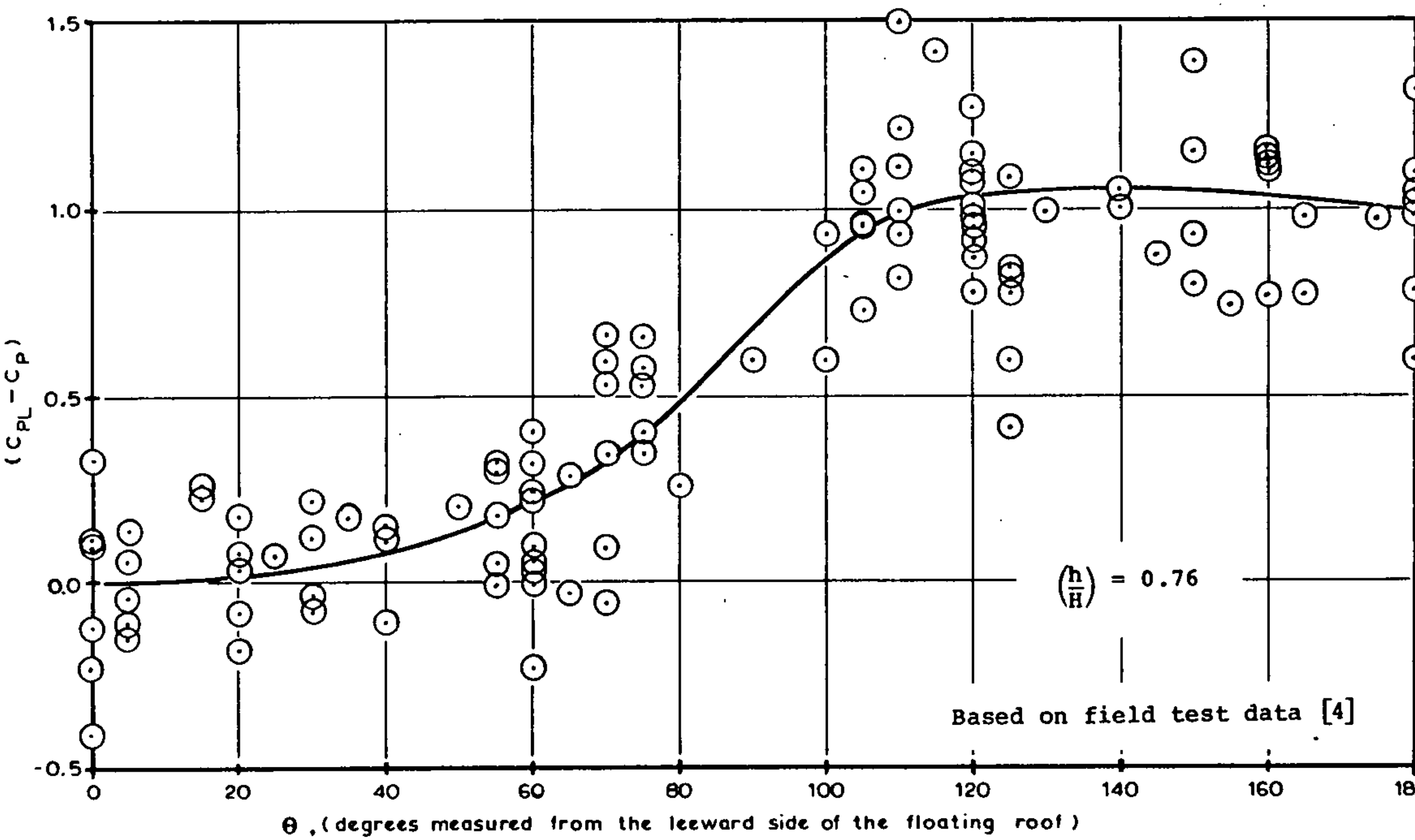

Figure 5 - Pressure Coefficient Difference ($C_{PL}-C_P$) Versus Location Above the Floating Roof Seal From Field Measurements

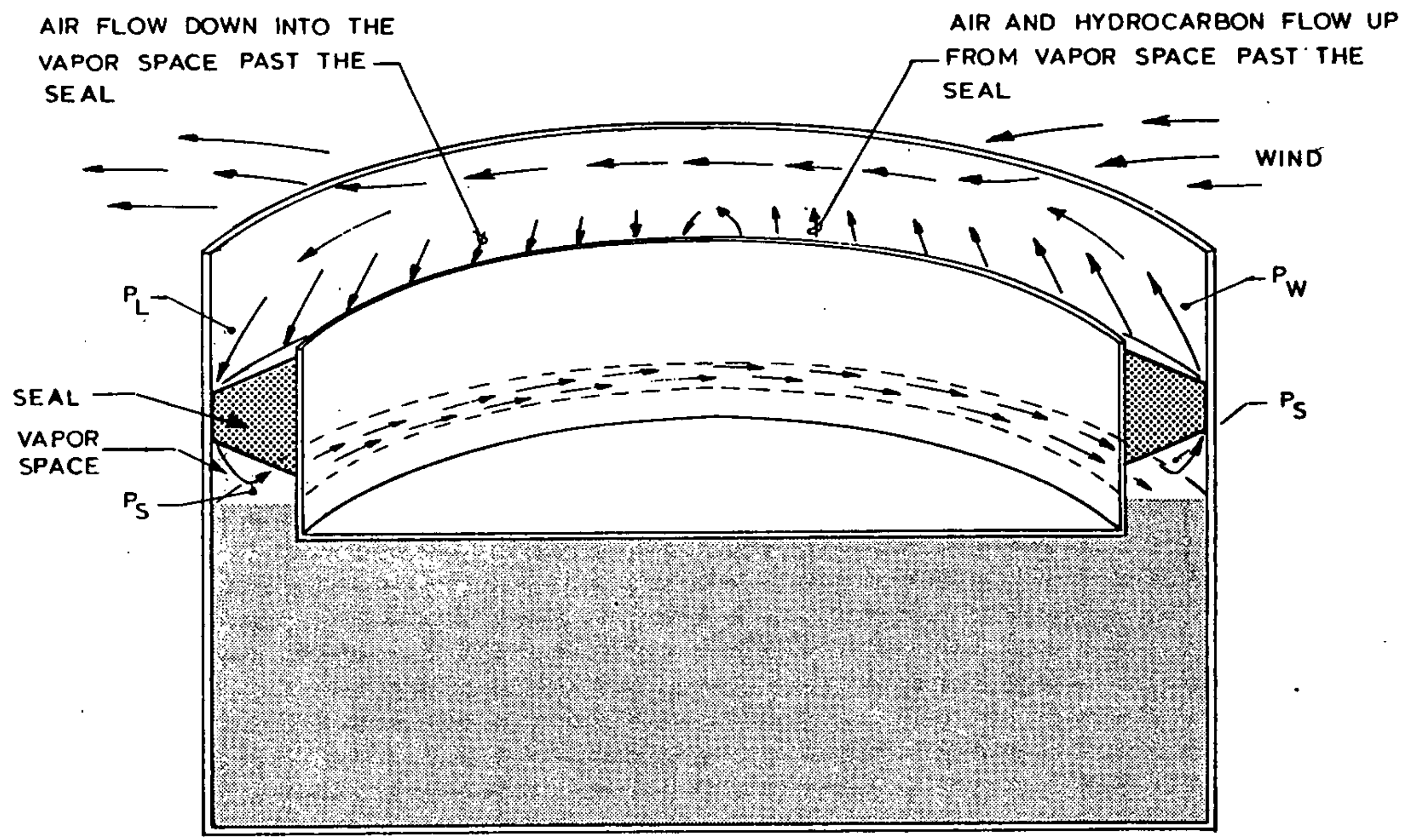

Figure 3 - Wind Induced Flow Effects on a Vapor-Mounted Seal

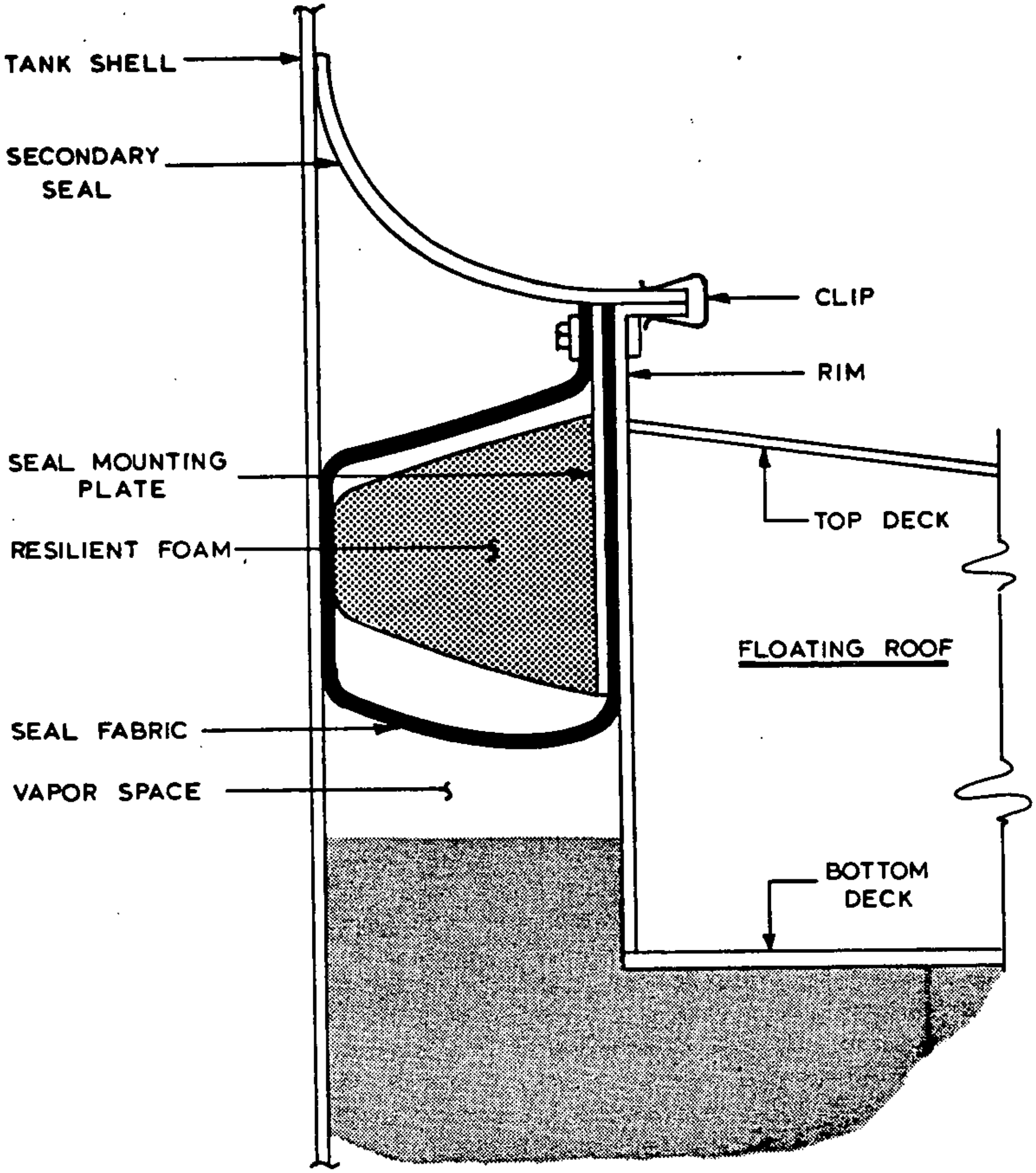

Figure 7 - Nonmetallic Vapor-Mounted Primary Seal (CBI Type SR-9 Resilient Foam Fabric Seal) With A Rim-Mounted Secondary Seal

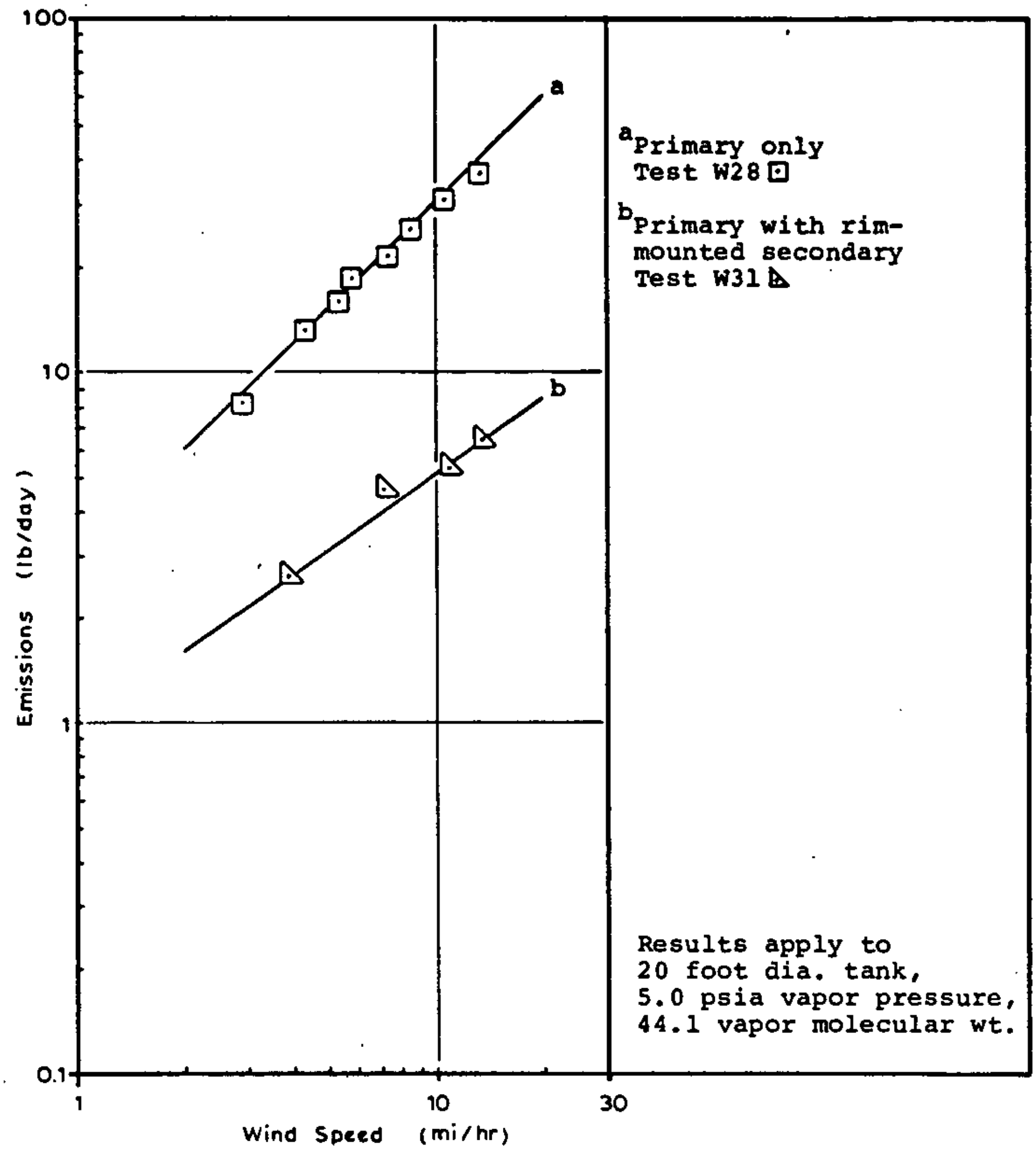

Figure 9 - Riveted Tank With Metallic Primary Seal

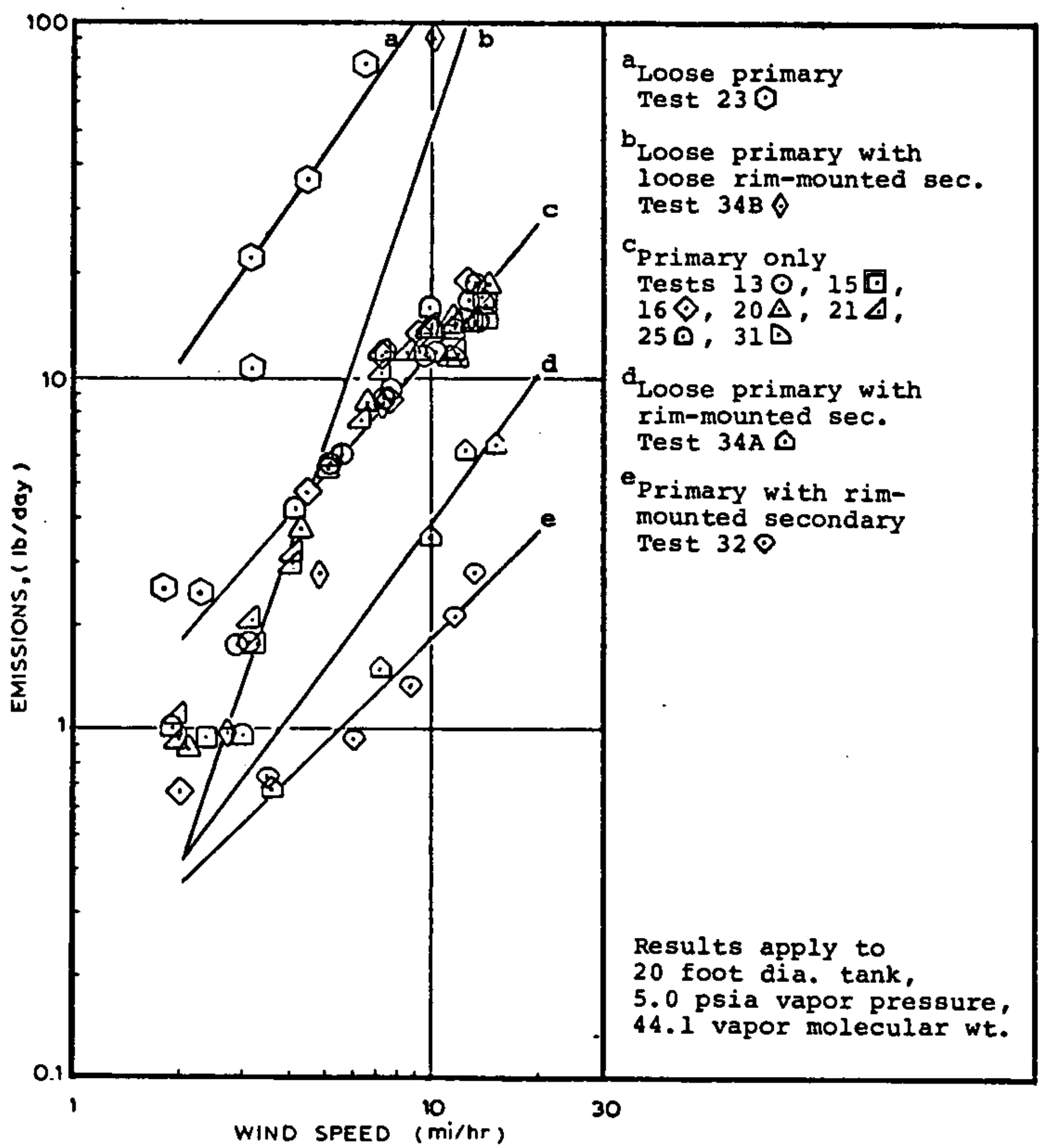

Figure 11 - Welded Tank With Vapor-Mounted Nonmetallic Primary Seal

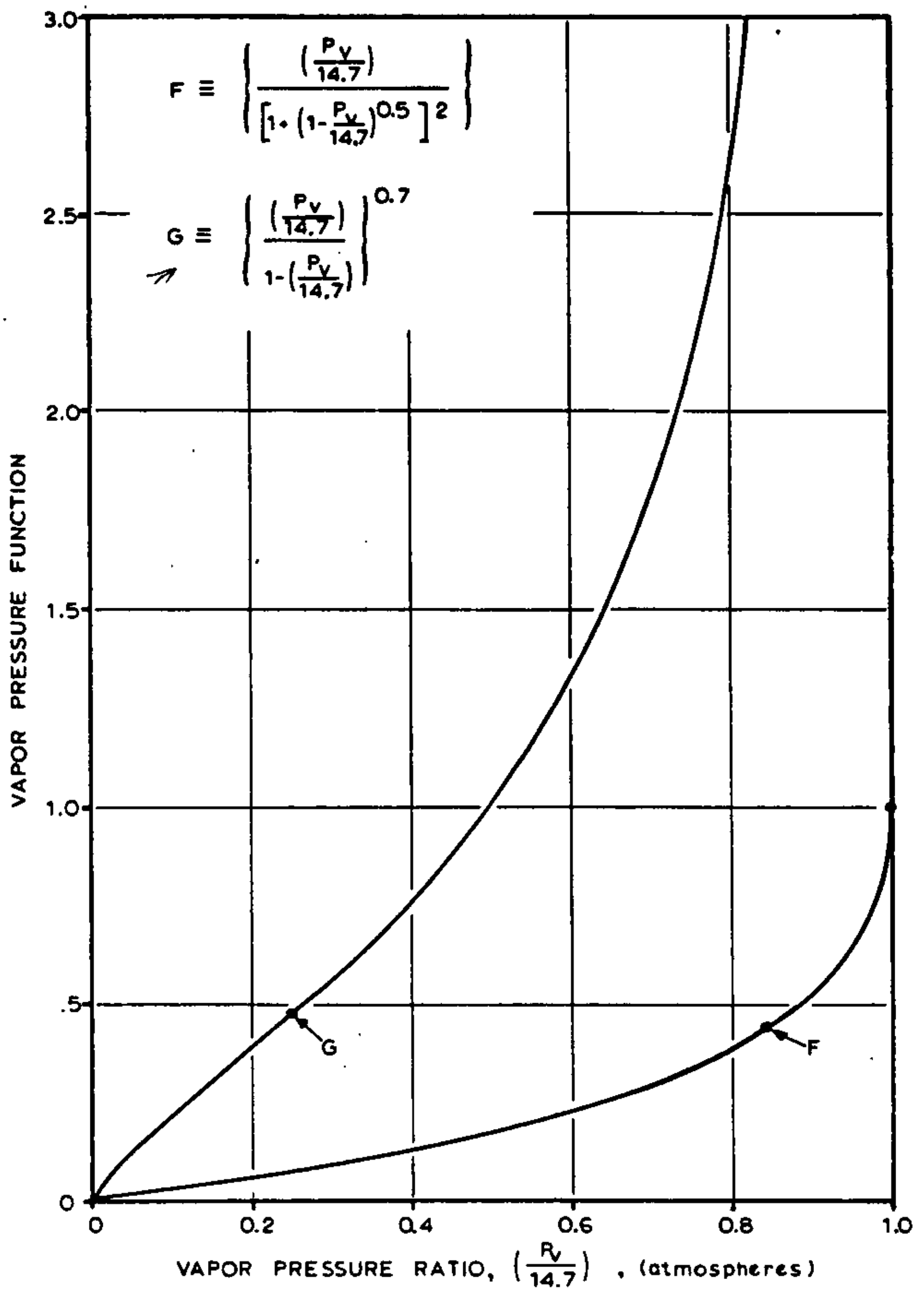

Figure 13 - Comparison of Vapor Pressure Function F and G

Table 1 - Summary of Gap Conditions

Case No.[a]	Primary Seal: Seal Type[b]	Primary Seal: Nominal Gap Description	Primary Seal: (Gap Area / Tank Dia) (in²/ft)	Secondary Seal: Seal Type[b]	Secondary Seal: Nominal Gap Description	Secondary Seal: (Gap Area / Tank Dia.) (in²/ft)	Test No.
1.1	A	Rivets	39.2	none	-	-	W28
1.2	A	Rivets	39.2	B	Rivets	1.8	W31
2.2	A	4-1½" x 72" Lg.	13.3	none	-	-	W26
2.4	A	No gaps	0	C	Various sizes	0.4	C1
2.6	A	1-½" x 377" Lg.	9.4	B	No gaps	0	W7
2.7	A	1-½" x 377" Lg.	9.4	B	2-½" x 24" Lg.	1.3	W8
3.3	D	2-½" x 24" Lg.	1.0	B	No gaps	0	34A
3.4	D	2-½" x 24" Lg.	1.0	B	2-½" x 24" Lg.	1.0	34B
4.2	E	4-½" x 24" Lg.	2.6	none	-	-	C36, C38
4.3	E	4-½" x 24" Lg.	2.6	F	-	-	C35
4.4	E	4-½" x 24" Lg.	2.6	B	No gaps	0	C31
4.5	E	C	14.1	B	4-½" x 24" Lg.	2.6	C32

[a]Only those cases from Table 2 which had intentional gaps installed are listed.

[b]Seal types denoted as follows:
A. Metallic shoe primary seal, CBI Type SR-1
B. Flapper secondary seal, Mayflower Type
C. Shoe-mounted wiper secondary seal, CBI Type
D. Vapor-mounted, nonmetallic primary seal, CBI Type SR-9, Flexible Foam Fabric Seal
E. Liquid-mounted, nonmetallic primary seal, CBI Type SR-5, Liquid Filled Fabric Seal
F. Weather shield installed

[c]The primary seal was gapped 1/8" for 60% of the tank circumference; 1/2" for 30%; and 1½" for 10%.

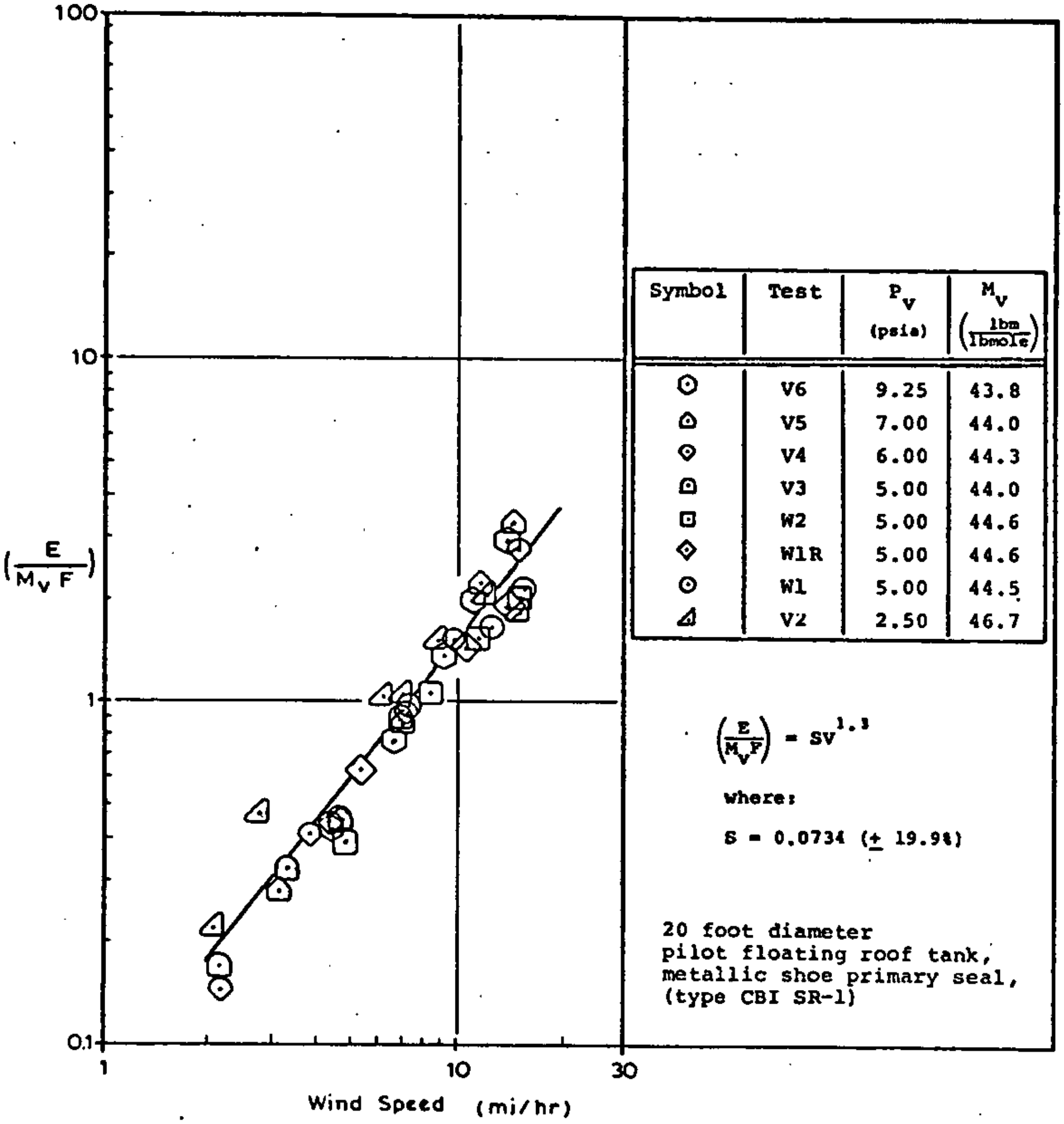

Figure 15 - Emission Correlation Versus Wind Speed For Various Vapor Pressures

Table 2 - Summary of K_s and n Factors

Case No.	Tank and Seal Type	K_s	n	Reference Test No.
1.0	Riveted tank with metallic primary seal			
1.1	Primary only	12.0	1.0	W28
1.2	Primary with rim-mounted secondary	4.0	0.7	W31
2.0	Welded tank with metallic primary seal			
2.1	Primary only	1.2	1.3	W1, W1R, W2, V3
2.2	Loose primary	2.5	1.3	W26
2.3	Primary with shoe-mounted secondary	1.0	1.0	C2
2.4	Loose primary with loose shoe-mounted secondary	2.0	0.9	C1
2.5	Primary with rim-mounted secondary	0.8	0.3	W10
2.6	Loose primary with rim-mounted secondary	1.5	0.4	W7
2.7	Loose primary with loose rim-mounted secondary	1.5	0.6	W8
3.0	Welded tank with vapor-mounted nonmetallic seal			
3.1	Primary only	3.0	1.2	13, 15, 16, 20, 21, 25, 31
3.2	Loose primary seal	15.0	1.5	23
3.3	Primary with rim-mounted secondary	0.7	1.0	32
3.4	Loose primary with rim-mounted secondary	0.6	1.4	34A
3.5	Loose primary with loose rim-mounted secondary	0.2	3.0	34B
4.0	Welded tank with liquid mounted nonmetallic seal			
4.1	Primary only	0.7	0.9	C29
4.2	Loose primary seal	2.3	0.9	C36, C38
4.3	Loose primary with weather shield	1.1	0.9	C35
4.4	Loose primary with rim-mounted secondary	1.2	0.5	C31
4.5	Loose primary with loose rim-mounted secondary	4.2	0.6	C32